

Messaging-based Intelligent Processing Unit (m-IPU) for next generation AI computing

Md. Rownak Hossain Chowdhury and Mostafizur Rahman, *Senior Member, IEEE*

Abstract—Recent advancements in Artificial Intelligence (AI) algorithms have sparked a race to enhance hardware capabilities for accelerated task processing. While significant strides have been made, particularly in areas like computer vision, the progress of AI algorithms appears to have outpaced hardware development, as specialized hardware struggles to keep up with the ever-expanding algorithmic landscape. To address this gap, we propose a new accelerator architecture, called messaging-based intelligent processing unit (m-IPU), capable of runtime configuration to cater to various AI tasks. Central to this hardware is a programmable interconnection mechanism, relying on message passing between compute elements termed Sites. While the messaging between compute element is a known concept for the Network on Chip or multi-core architectures, our hardware can be categorized as a new class of coarse-grained reconfigurable architecture (CGRA) specially optimized for AI workloads. In this paper, we highlight m-IPU’s fundamental advantages for machine learning applications. We illustrate the efficacy through implementations of a neural network, matrix multiplications and convolution operations, showcasing lower latency compared to state-of-the-art. Our simulation-based experiments, conducted on the TSMC 28nm technology node, reveal minimal power consumption of 44.5 mW with 94200 cells utilization. For 3D convolution operations on (32 X 128) images, each (256 X 256), using a (3 X 3) filter and 4096 Sites at a frequency of 100 MHz, m-IPU achieves processing in just 503.3 milliseconds. Additionally, m-IPU delivers a throughput of 142.45 million images/second for small neural network comprising one convolution layer, one pooling layer, and two fully connected layers processing 20K 5X5 images at 1 GHz frequency utilizing only 48 SiteOs. These results underscore the potential of m-IPU as a unified, scalable, and high-performance hardware architecture tailored for future AI applications.

Index Terms—Machine Learning, Hardware Accelerator, Matrix Multiplication, Convolution, Reconfigurable Computing.

I. INTRODUCTION

The advent of Artificial intelligence (AI), particularly Deep Neural Networks (DNNs) has prompted a paradigm shift in various fields such as computer vision, natural language processing, robotics, and many more. As a result, modern tech industries are aggressively integrating advanced neural network architectures like AlexNet [1], VGGNet [2], GoogLeNet [3], ResNet [4], LSTM [5], GRU [6], Transformers [7] to uplift customer experience and maintain a competitive edge. However, the fast-paced advancements and escalating computational demands of AI have exposed significant limitations in traditional computing systems, especially as Dennard’s scaling becomes obsolete [8] and Moore’s law nears its end [9]. This spurs innovation in designing specialized hardware architecture tailored to application domains, rather than merely optimizing existing ones [10], ushering in a new

era of domain-specific computer architecture development to improve performance persistently[11].

Recent years have witnessed substantial research efforts aiming at efficient of processing AI workloads. As a result, several specialized hardware accelerators, such as TPU[12], MEISSA[13], SpArch[14], MatRaptor[15], CGRA-based Inference Engine [16] have emerged to address the growing demands of computationally intensive AI tasks. While these architectures do outperform traditional CPU and GPU architectures, they lack generality in terms of application. Reconfigurability either in logic or routing capabilities is essential to map the variety of AI algorithms that are emerging.

In this study, we present a novel programmable hardware architecture distinguished by its messaging-based interconnection system. The m-IPU’s configurability stems from its flexible interconnections, which facilitate the spontaneous mapping and processing of large data volumes via a message-passing scheme, eliminating the need for host processor intervention. In conjunction with this innovative computing framework, we have optimized the hardware design at the micro-architectural level to enhance overall performance. Our hierarchical and modular design approach ensures a scalable architecture that can adapt to the evolving demands of AI applications. Consequently, our matrix multiplication method utilizing the m-IPU engine exhibits lower latency compared to state-of-the-art designs such as MEISSA and TPU, while also enabling high throughput for convolution operations through messaging-based intelligence. The key contributions of this paper are as follows:

- Details of the mIPU architecture and its contrast with TPU and other reconfigurable architectures such as FPGA and CGRA.
- Mapping of AI tasks such as matrix multiplication, convolution operation in m-IPU.
- Architecture evaluation through synthesis and emulation at TSMC 28nm technology node.
- Comparison of key performance metrics with other architectures

This paper is organized as follows. Section II reviews the prior works in reconfigurable hardware architecture domain and highlights the motivation to develop specialized hardware tailored for AI applications. Section III delves into the m-IPU architecture with system-level overview and demonstration of hardware hierarchy. Next, Section IV outlines the methodology for performing matrix multiplication and convolution operations, describing the data mapping strategy within the m-

IPU fabric. Section V elaborates on the implementation set up to validate our design under TSMC 28nm technology and highlights record performance of key design metrics such as resource utilization, power profile, latency, and throughput. This section also provides a comparative analysis with other cutting-edge architectures. Finally, section VI summarizes the concluding remarks emphasizing key contributions of the m-IPU.

II. PRIOR WORK & MOTIVATION

The merit of an AI accelerator hinges on the balance between its efficiency and flexibility. Hence, the performance of an AI accelerator lies in its ability to support diverse AI models ensuring high throughput and energy optimization across a wide range of neural network configurations [20]. This trade-off has driven AI accelerator research towards two distinct computing paradigms: a) Reconfigurable computing and b) Task specific Specialized computing. Specialized architectures are highly optimized for dedicated tasks, but they often fall short in addressing the broader spectrum of application requirements. For instance, SpArch and MatRaptor are fine-tuned for highly sparse networks like the Amazon co-purchase network[21], while MEISSA leads in low-latency tasks in edge devices like autonomous drones[22], and TPUs dominate high-throughput scenarios like data centers[12]. Despite their strengths, this rigid application-centric approach will lead to shorter lifecycles and higher nonrecurring engineering costs while deploying different AI workloads[23][24].

In contrast, reconfigurable architectures provide the required flexibility, to dynamically adapt hardware for various computational tasks[25]. Hence, several reconfigurable computing concepts like Coarse-Grained Reconfigurable Architectures (CGRAs)[26], Field-Programmable Gate Arrays (FPGAs)[27], memristor-based reconfigurable circuit[28], fine-grained polymorphic circuit[29], noise-based configurable computing[30], crosstalk built-in memory [31] have been introduced to enhance the computational capabilities. While specialization enhances efficiency, incorporating reconfigurability often incurs architectural overhead. For example, FPGAs offer fine-grained reconfigurability at the logic gate level, allowing virtually any kind of circuit to be implemented, but suffer from slower clock speeds and longer configuration times[32]. CGRAs, on the other hand, balances between flexibility and specialization by offering a coarser-grained reconfiguration, positioning themselves as a middle ground between FPGAs and more rigid, highly specialized ASICs[33].

CGRAs are specifically designed for data-parallel tasks such as digital signal processing, image processing, and machine learning, utilizing an array of processing elements (PEs) that can be reconfigured for specific operations[34]. However, despite their versatility, CGRAs pose significant deficiencies when applied for machine learning or data analytics tasks. For example, the CGRA-based VersatCNN architecture[35], while designed to provide efficient acceleration for CNN inference in embedded systems, faces

several limitations. The frequent reconfiguration required for different CNN layers and operations, controlled by multiple address generator units (AGUs), introduces significant overhead, particularly during transitions between convolution, max-pooling, and up sampling layers. This reconfiguration process, although flexible, impacts real-time performance. Additionally, the fixed parallelism of 832 MAC units is optimized for certain layers but may lead to underutilization in layers with fewer computations or more irregular dataflows, reducing overall efficiency [36]. Furthermore, while convolution layers are highly optimized, non-convolutional operations such as post-processing routines (e.g., object detection box drawing) and control-heavy functions remain handled by the RISC-V CPU, limiting the speedup potential. These limitations affect the architecture's adaptability to more diverse and complex workloads, ultimately restricting its scalability across varying CNN models.

The CGRA-based EMAX architecture proposed by Tanomoto et al. [37] is centered around a grid of PEs, each containing fixed 32-bit, 2-stage floating-point units (EX1, EX2), FIFOs, and local memory to facilitate parallelism. However, the fixed nature of the execution units leads to inefficiencies when dealing with complex or irregular tasks, such as non-linear activations and pooling operations, resulting in underutilization of hardware resources [38]. The static configuration, although allowing flexible mapping of operations, lacks dynamic reconfigurability, further limiting the system's ability to adapt to diverse and evolving CNN tasks[39]. Moreover, while pipeline parallelization is implemented for both forward and backward propagation, the fixed PEs and the double-buffering mechanism introduce synchronization delays, particularly in convolutional layers with larger kernels, ultimately causing bottlenecks that slow down overall performance in deeper neural networks.

Yin et al. [40] present a reconfigurable hybrid-neural-network processor that achieves energy efficiency of 1.06-to-5.09 TOPS/W for deep learning applications, but its limitations stem from performance trade-off between energy consumption and speed[41]. The processor operates at lower frequencies, as low as 10MHz in certain modes, sacrificing real-time performance and throughput for energy savings. Additionally, it relies on low-precision (8-16 bit) computations, making it less suitable for tasks that require 32-bit precision, such as model training. The architecture's use of heterogeneous processing elements, which enable specialized operations like pooling and RNNs, adds complexity, necessitating dynamic partitioning of processing elements (PEs). This partitioning, controlled by an external host, incurs significant overhead, limiting the processor's adaptability in real-time environments.

The Eyeriss architecture[42], though optimized for energy efficiency, encounters limitations related to its reconfiguration and data movement mechanisms. The 1794-bit scan chain used for reconfiguring the system between CNN layers introduces overhead and limits real-time adaptability, making the architecture less effective in deep networks requiring frequent reconfiguration[43]. The Network-on-Chip (NoC) effectively reduces off-chip data movement but struggles with

synchronization delays during the processing of larger convolutional layers, such as in VGG-16, resulting in reduced throughput[44]. These limitations, including reconfiguration overhead, synchronization bottlenecks in the NoC constrain Eyeriss's scalability and performance when applied to more complex and computationally demanding neural network architectures.

Given these constraints, future AI hardware architectures require innovative, runtime-reconfigurable computing solutions, which the messaging-based intelligent processing unit (mIPU) aims to fulfill. In mIPU, each message encodes both the current and next opcodes, along with spatial addresses and the corresponding data. This encoding allows the underlying hardware to not only execute the immediate tasks but also inherently set up future configurations. While domain-specific AI accelerators like Google's Tensor Processing Unit (TPU) are optimized for specific computations (e.g., Multiply and Accumulate) within fixed data flows (systolic arrays for matrix multiplication)[12], the mIPU stands apart by offering dynamic reconfigurability. mIPU leverages an agile message-passing system where data routes based on message content, enabling the architecture to handle varied data dimensions and flows. Moreover, its internal message generation and propagation mechanism further reduce expensive memory read operations and data movement, enabling mIPU in adapting to diverse AI workloads, overcoming the limitations of specialized accelerators.

The micro-architecture of mIPU, like CGRAs, organizes its computational units in a 2D grid. However, unlike CGRAs, which are designed to cater to a wide variety of applications, mIPU is purpose-built to map various AI operations like convolution, RELU and pooling. This makes mIPU a domain-specific, self-reconfigurable hardware accelerator with a focus on AI tasks, while still retaining certain traits like domain-agnostic CGRAs. Moreover, m-IPU distinguishes itself from CGRA in its execution model to achieve reconfigurability. In CGRAs, processing elements are configured either statically [45][46][47][48] (at compile time) or dynamically

[49][50][51][52] (based on runtime states), where operations are either executed in a predefined order or based on operand readiness. But this approach restricts CGRAs adaptability in AI applications that requires frequent real-time adjustments. For example, autonomous driving demands continuous decision updates from real-time sensor input, while NLP tasks require swift adjustments to accommodate evolving model architectures during execution[53]. In contrast to CGRAs, mIPU embeds both present and future execution instructions within each message, inherently enabling continuous reconfiguration without external intervention. Thus, m-IPU allows for seamless task management on-the-fly, offering more agility and faster reconfiguration than CGRAs, which often struggle with real-time adjustments and dynamic workloads.

Another key distinction of mIPU with other architectures lies in its flexible interconnection mechanisms. The microarchitecture of mIPU employs a runtime message-passing strategy, where messages flow between neighboring computational elements via interconnected pathways and through adjacent tiles using a fine-grained hierarchical bus structure. Unlike network on chips (NoCs), which rely on predefined pathways and routing algorithms to optimize data flow[54], m-IPU's message-driven routing paths enables flexible, real-time data transfer. This dynamic, message-driven system not only simplifies data flow management but also minimizes hardware overhead. By minimizing the interconnection architecture, mIPU allows for a greater number of computational units to be integrated, enhancing parallelism and achieving higher throughput— areas where rigid NoC structures often fall short.

III. M-IPU ARCHITECTURE

Messaging based Intelligent Processing Unit (mIPU) is a reconfigurable computing architecture whose computing and memory elements are parallel and distributed. The cornerstone of our programmable hardware architecture is flexible virtual interconnections, which is pivotal for integrating messaging-

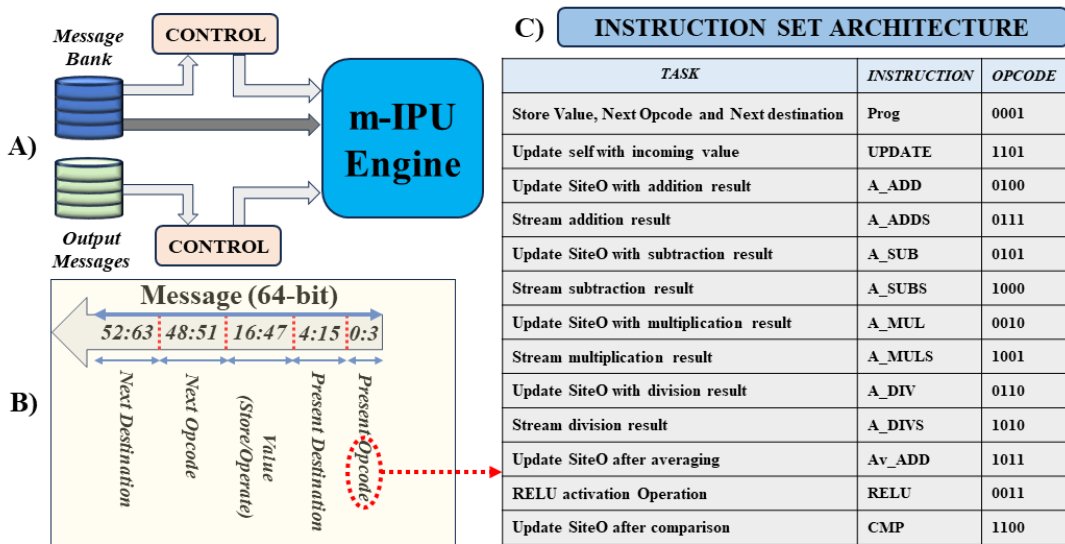


Figure 1 A) System Overview B) Message Encoding Scheme C) Instruction Set Architecture of m-IPU.

based intelligence and thereby enabling efficient information processing. The proposed interconnect configuration is analogous to message passing in a human chain[55]. For instance, if there are 5 people in a line and they want to pass messages from person #1 (Source) to person #5 (Destination), then persons #2, #3, and #4 form a virtual link between source and destination in that message passing scheme. This source, destination-based message passing scheme can be applied to computing cores as well. The m-IPU, leveraging this source-destination based message passing mechanism can behave as a custom-ASIC at runtime for each running AI applications to deliver the best performance.

A system overview of the m-IPU is depicted in Figure 1(A). Here, a host CPU is required (like GPUs and other accelerators) to interpret high-level language (e.g., C, Python, etc.) and translate them into messages that m-IPU can operate upon and collect outputs form the m-IPU. Inside the m-IPU all communication between computing elements is performed through messages. The encoding scheme of a 64-bit message in m-IPU is shown in Figure 1 (B). A message can be segmented

generate new message. To program m-IPU on-the-fly, we developed a lightweight instruction set architecture (ISA) as shown in Fig. 1(C) comprising only 13 instructions.

A. Hardware Details

The m-IPU follows a modular and hierarchical design approach enabling it to be scalable irrespective of data size or model complexity. The construction and segmentation of the m-IPU architecture is outlined in Figure 2 (A-E). Inside the m-IPU engine, there is an array of Quads. A Quad is a collection of 4 Blocks, and a Block is a collection of 16 Tiles. Each Tile consists of 16 SiteMs and each SiteM incorporates 16 SiteOs. The Quads, Blocks, Tiles, and SiteMs hierarchy allows task distribution and parallel computing. The SiteOs are the core elements and are analogous to Threads of GPUs or the Processing Elements (PEs) of TPUs. SiteOs are organized in rows and columns and the programmable interconnections between SiteOs allows the messages to be routed any cores. A SiteM collects all these messages and outputs 12 messages (4 for its own Tile, 4 for other Tiles within the same row, and 4 for different columns/Blocks) at a time. Like SiteMs organization

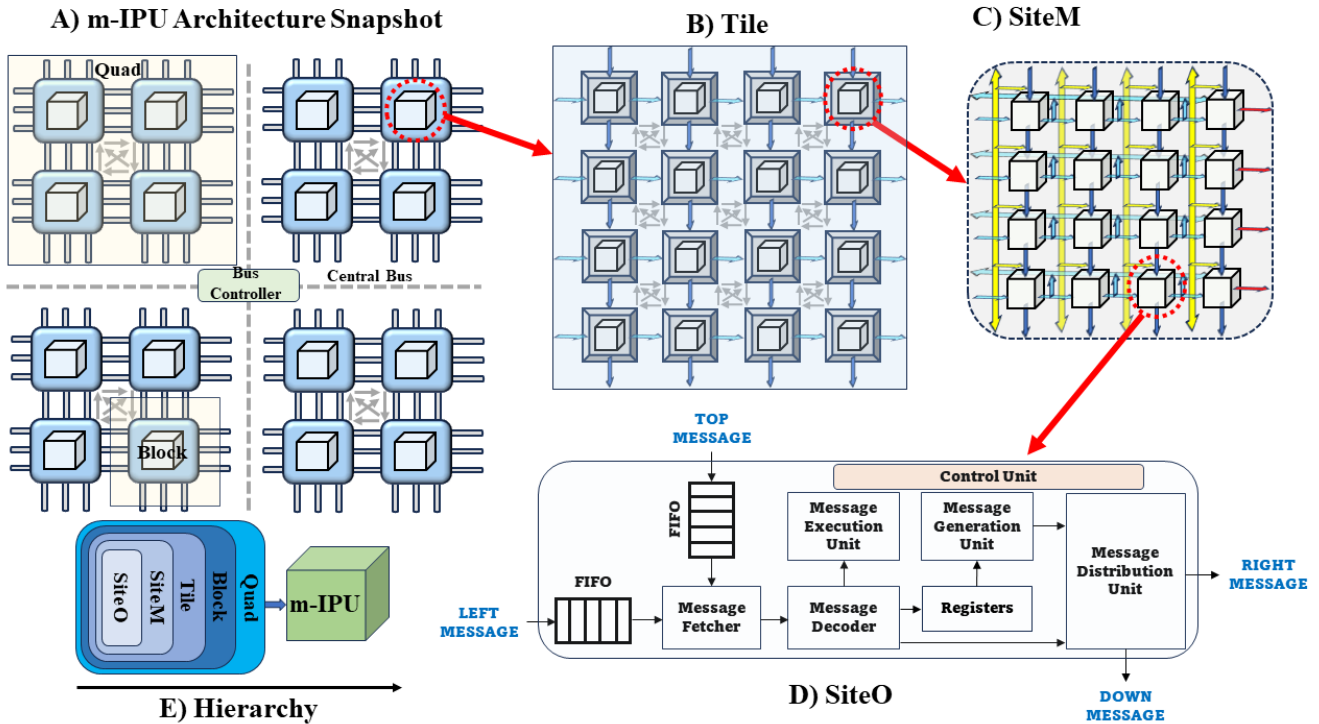


Figure 2 Details of A) m-IPU architecture B) Tile C) SiteM D) SiteO E) Hierarchy

into 5 parts: a) Present Opcode (from bit position 0 to 3), b) Present Destination (from bit position 4 to 15), c) Values to be stored / operated (from bit position 16 to 47), d) Next Opcode (from bit position 48 to 51), and e) Next Destination (from bit position 52 to 63). In this framework, messages are routed to the desired hardware unit within the m-IPU based on the Present Destination, where an operation is performed on the value embedded in the message according to the Present Opcode. Subsequently, the Next Opcode and Next Destination specified in the message are retained inside the m-IPU to

in a Tile, a collection of Tiles is called Blocks. The Blocks communicate with each other through local and global buses. Each block also contains distributed embedded memory elements to store further instructions.

The fundamental computing core of the m-IPU is SiteO, which is responsible for both computation and message passing. The hardware architecture of SiteO as shown in Figure 2(D) mainly comprises floating point unit (FPU), FIFO, decoder, counter, and register. Associated with each SiteO there is a small 8-word memory buffer to store the next set of

instructions. The SiteOs also contain SRAMs to store weights. The SiteOs execute 32-bit IEEE 754 arithmetic operations, such as addition, multiplication, and subtraction, utilizing the Floating-Point Unit (FPU). SiteOs can receive messages either from the top or the left direction and they release outputs either at the right or the bottom direction. They are also aware of their neighbors (i.e., addresses of neighbor SiteOs in right, left, up, and down are stored in each SiteO). There are 2 FIFOs (Left and Top) to store incoming messages and push them towards execution or exit route in a pipelined manner. If the FIFOs are empty, the turnout time for in and out for a message is 1 cycle. If the FIFOs are full, the senders are sent a full signal to stop sending. The phase when stationary values are first loaded is called programming. The instruction set architecture for the m-IPU is depicted in Figure 1 (c), and a set of messages for an example neural network is detailed in the Table IV of the appendix section as supplementary file.

When a message arrives at SiteO, it first checks whether the destination of the message is its address, and if it matches, then the message is decoded and the instruction embedded within the message is executed, otherwise, the message is passed on. After decoding a message, a SiteO can perform either message streaming or message forwarding. Streaming and forwarding are two different tasks; in the case of streaming, the SiteO receiving the message send it to its preferred neighbor by updating the message, whereas, in forwarding, the SiteO just behaves as a buffer to pass messages without intervention. Each Site, upon receiving or generating a message, checks whether the destination is within the same row or not; if it is, then it sends the message to the right and to down otherwise. Eventually, through hopping Sites, a message reaches its destination. If the messages are to be routed/passed downward, those messages are labeled as Tile message and if they are

passed rightward (within the same SiteO row), those are labeled as Local messages. To serve two different purposes such as Data loading and mathematical operation, m-IPU needs just 13 instructions. Here, 1 instruction (*Prog*) is required for loading data inside m-IPU and the remaining 12 instructions (*UPDATE, A_ADD, A_ADDS, A_SUB, A_SUBS, A_MUL, A_MULS, A_DIV, A_DIVS, Av_ADD, RELU, CMP*) perform mathematical operations.

A SiteM is designed arranging 16 SiteOs in rows and columns. Each column and row of the SiteM is equipped with four vertical and horizontal buses, respectively. The bus topology enables messages to be dispatched simultaneously at multiple SiteO locations rather than hopping thereby improving latency. This concept can be mimicked and extended to develop other hierarchical structures like tile, block, and quad. A Tile can have messages destined to itself (i.e., coming from within the Tile or outside the Tile), called Tile messages, and have incoming messages destined for other Tiles within the same row (called Local messages with respect to Blocks) and same column (called Block messages).

IV. M-IPU COMPUTATION

Matrix multiplication and convolution operations are key computational kernel in various state-of-the-art AI applications. Hence, the performance of AI accelerators lies in the efficient execution of matrix multiplication and convolution operations. As AI technology advances, the complexity of neural networks continues to increase. For example, CNN architectures encompass multiple layers with varying filter size, padding, and stride to convert input image volume to output preserving class scores[56]. Ideally, the convolution operation is a repetitive sliding dot product according to filter size. However, this

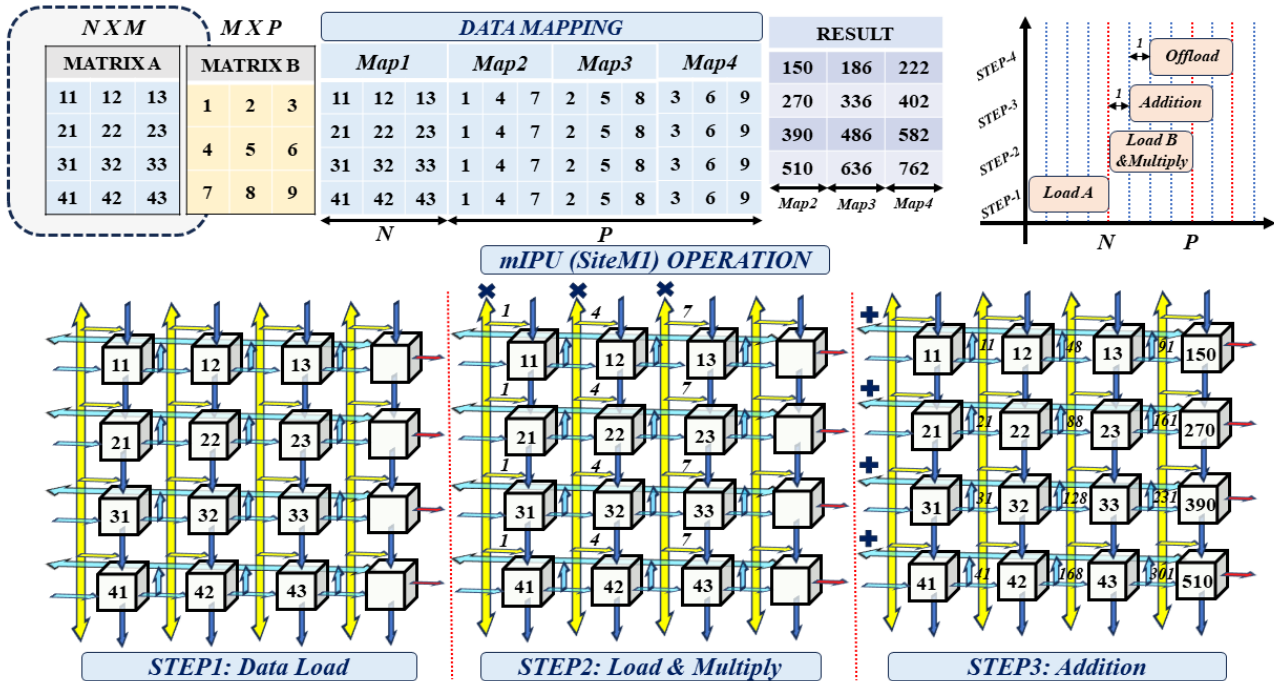


Figure 3 Matrix Multiplication Approach in m-IPU.

conventional approach requires many operations to be performed; hence, effective data mapping is parallelly significant along with efficient hardware architectures to accelerate convolution operations. Moreover, the performance metrics and data processing capabilities of convolution operation vary according to the application. Real-time systems such as autonomous vehicles[57], smartphones[58], medical devices[59], robotics [60] necessitates instant decision making based on sensory inputs. However, due to resource limitations, they are capable of single-batch processing; hence, the key design parameter in those applications is latency. On the other hand, applications like video processing[61], language modeling[62], speech recognition 0 process multiple batches at the same time; as a result, requires high throughput. This section will explore both the matrix multiplication and convolution operations in m-IPU, catering to the varying needs of these AI applications.

A. Matrix-Matrix Multiplication

The matrix multiplication operation inside m-IPU can be divided into four steps: a) Data (Matrix A) Load, b) Data (Matrix B) Load and multiply, c) Addition, and d) Offload. Figure 3 illustrates a matrix-matrix multiplication example within mIPU utilizing a SiteM. Here, the inputs for the matrix multiplication are Matrix A (4 X 3) and Matrix B (3 X 3). According to the data mapping indicated in Figure 3, matrix A will be loaded only once following Map1. After that, each column of the matrix B will be loaded sequentially according to Map2, Map3, and Map4. Thus, the matrix multiplication can be surmised as three (3) matrix-vector multiplication operations. Therefore, the matrix-vector multiplication between matrix A and each column of matrix B will be repeated 3 times in one

SiteM. The corresponding result of each matrix-vector multiplication will be accumulated to achieve the final output. Alternatively, the intended multiplication operation can also be completed using 3 SiteM fabrics of the m-IPU; where, 3 SiteMs will perform 3 matrix-vector multiplications parallelly in 3 SiteMs. Thus, the matrix-matrix multiplication can be acquired within the same time of matrix-vector multiplication using 3 SiteMs. Mathematically, the number of SiteOs and the latency needed to execute a matrix-matrix multiplication of Matrix A (N X M) and Matrix B (M X P) can be calculated using the equation (1) and (2) respectively.

$$SiteO_{MM} = \{(N \times X \times M) + N\} \times P \tag{1}$$

$$T_{MM} = N + P + 2 \tag{2}$$

B. Convolution Neural Network

To illustrate the functionality of a convolutional neural

TABLE I
Network Configuration and performance of an Example Convolutional Neural Network considered for illustration

NETWORK CONFIGURATION						
Layer	Feature Map	Size	Kernel Size	Stride	Activation	
IN	Image	1	5X5	-	-	-
2	Conv	4	3X3X4	3X3	0	RELU
3	Pool	4	2X2X4	2X2	1	RELU
4	FC	-	16	-	-	RELU
OUT	FC	-	4	-	-	SOFTMAX

HARDWARE PERFORMANCE (Precision FP32)				
#SiteOs	Freq. (GHz)	Batch	Images/ Batch	Throughput (Images/Second)
48	1	1	20000	142.45 X 10 ⁶

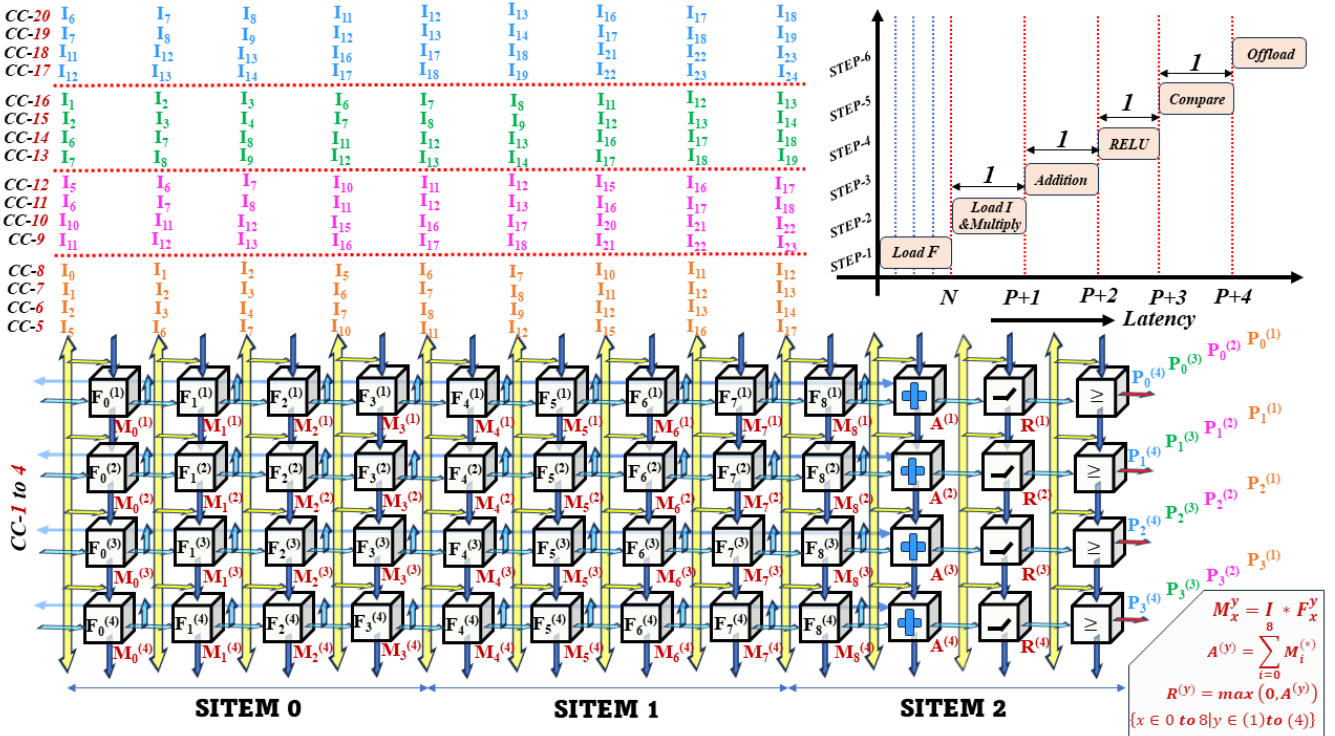


Figure 4 Data mapping for Convolutional Neural Network (CNN) in m-IPU.

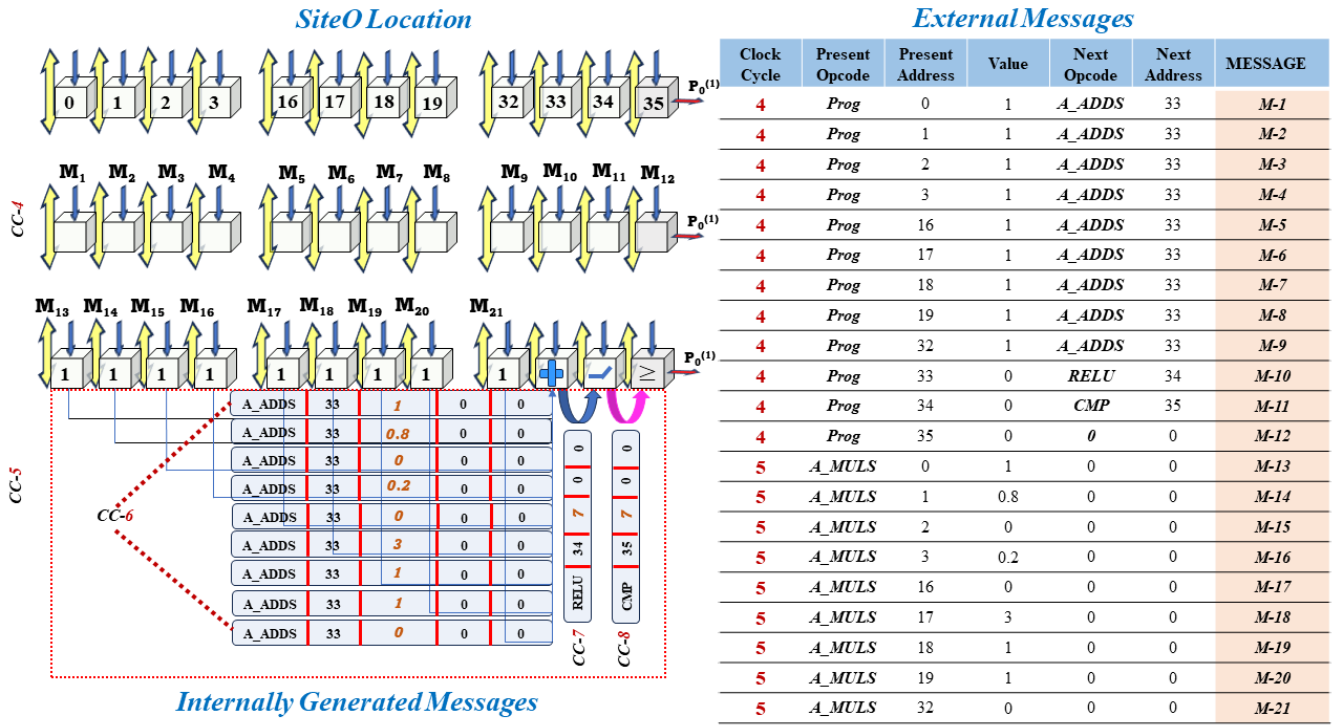


Figure 5 Demonstration of messaging-based computation for Convolution Layer in m-IPU.

network (CNN) within the mIPU architecture, we consider a simple network configuration. This network involves processing a 5x5 single-channel image through a series of layers, starting with a convolution layer equipped with four 3x3 filters (using a stride of 1 and no padding), and followed by a 2x2 pooling layer (with a stride of 1) as shown in Table I.

The system employs 3 SiteMs (SiteM0, SiteM1, SiteM2) to manage all network operations. To optimize hardware performance, we have prudently analyzed CNN architecture’s behavior, aiming to devise an efficient mapping strategy. During weights loading, we prioritize data that must travel longer intra-fabric distances. This ensures such data is in place by the time data covering shorter distances is processed, thereby minimizing overall latency and improving synchronization across the computing nodes. Secondly, during convolution operation the same image is multiplied with different filter values; therefore, different filters are loaded into a single SiteM, allowing the same image values to be consistently transmitted via the vertical bus. Next, we strategically send specific image values to specific SiteMs to ensure maximum data reusability since every pooling values always depends on certain blocks of images. Even though this approach is doing some redundant operations, however, it does not deteriorate the performance significantly as all SiteMs are being operated parallelly.

The operational strategy for the convolutional neural network (CNN) can be divided into two main phases: i) Phase-1: Weights Loading, and ii) Phase-2: Operations, which include multiplications, additions, activations, and comparisons (max pooling). For the implementation of CNN operations, two distinct message types as listed in Table IV of the appendix section as supplementary file are utilized: i) Type-1, where the

present opcode is "Prog", responsible for weights loading, and ii) Type-2, where the present opcode is not "Prog", responsible for carrying out operational tasks. Each SiteM receives messages via two different routes: either through the top four ports of the respective SiteM or through the vertical bus. Data flow within the SiteM occurs through two primary mechanisms: i) Hopping, and ii) Vertical Bus. During hopping, data travels to the intended SiteO locations across multiple SiteOs, based on the address of the target SiteO location. In contrast, the vertical bus facilitates the routing of the same data to multiple SiteOs within the same SiteM. Data hopping proves advantageous during Phase-1 (Weights Loading), where each SiteO requires programming with distinct values. In Phase-2 (Operations), when identical values must be multiplied by different weights, data propagation incorporates the use of the vertical bus.

During Phase-1 (Weights Loading), Type-1 messages are dispatched through the top ports of the respective SiteM and then reach the intended SiteO locations via hopping. Consequently, the required SiteOs are programmed with the appropriate weights within 4 clock cycles (CCs), as all SiteMs operate in parallel, as illustrated in Figure 4. Post programming, each SiteO retains the next opcode and destination address embedded in the message in its internal register. Upon completion of Phase-1, Type-2 messages are simultaneously transmitted to the SiteMs via the vertical bus every clock cycle, initiating operations as dictated by the opcode. Following each operation, new messages are generated using the next opcode and destination stored within the register along with the operation results. Specifically, the initial operation involves multiplication, with the results from the SiteOs being transferred to the desired SiteO location for addition via the

horizontal bus. Subsequently, a new message for the RELU operation is internally generated. After executing the RELU operation, another message is prepared for the comparison operation. This sequence is repeated as necessary until all required comparisons are completed, culminating in the offloading of results to memory. All messages required to complete the convolution operation are included in Table IV of the Appendix section as supplementary file. A segment of this message sequence is depicted in Figure 5. During the 4th CC, twelve Type-1 messages (M1-M12) are dispatched to three SiteMs, targeting SiteO locations 0 to 3 for SiteM0, 16 to 19 for SiteM1, and 32 to 35 for SiteM2, assuming all values in a 3x3 filter are "1." Consequently, each SiteO stores the values, subsequent opcodes, and destinations according to messages M1 to M12. At the 5th CC, nine Type-2 messages (M13-M21) with the opcode "A_MULS" are sent, which multiply the incoming values with the previously stored weights, generating nine internal messages using the stored next opcode and destination. All these internal messages, sharing the same opcode (A_ADDS) and destination (33), are sent to SiteO 33 and aggregated at the 6th CC. SiteO 33, holding the next opcode (RELU) and destination (34), then generates a new internal message with the addition results, directing it to SiteO 34 during the 7th CC. Following the RELU operation, another internal message is generated and sent to SiteO 35 during the 8th CC, continuing the cycle.

V. VALIDATION

To validate our design, we have developed a digital design flow based on CAD tools under TSMC 28nm technology node. Initially, we designed the RTL/behavioral models of m-IPU and iteratively checked whether the RTL is free from linting errors

and whether the RTL is synthesis friendly. During the RTL code development, we utilized Xilinx Vivado platform for initial measurement and simulation. Later, we followed a digital design flow based on standard methodologies and CAD tools for implementing the mIPU design. We have used a high-performance compact mobile computing plus (CLN28HPC+) process from TSMC 28nm commercial PDK with 8 metal layers and supply voltage of 0.9V. Here, the RTL was verified for functional correctness. We have also performed property checking to verify the RTL implementation and that the specification matches. After that, we set the design environment, including the technology file and other environmental attributes. We have also defined the design constraints file for synthesis, usually called an SDC synopsys_constraints or dc_synopsys_setup file, specific to the synthesis tool. We have defined the environment by specifying operating conditions, wire load models, and system interface characteristics. Operating conditions include temperature, voltage, and process variations. Wire load models estimate the effect of wire length on design performance. System interface characteristics include input drives, input and output loads, and fan-out loads. Since the environment model directly affects design synthesis results, we have methodically constrained designs by describing the design environment, target objectives, and design rules. We also constrained timing and area information and iteratively run the synthesis on the design to meet the design specifications. Once the constraints file is set, we have provided synthesis inputs to the Cadence Genus. The input files are the library files (which have the functional/timing information available for the standard cell library and the wire load models for the wires based on the fan-out length of the connectivity), RTL files, and the design constraints files. The synthesis tool performs the synthesis of the RTL files and maps and optimizes them to meet the design constraints requirements.

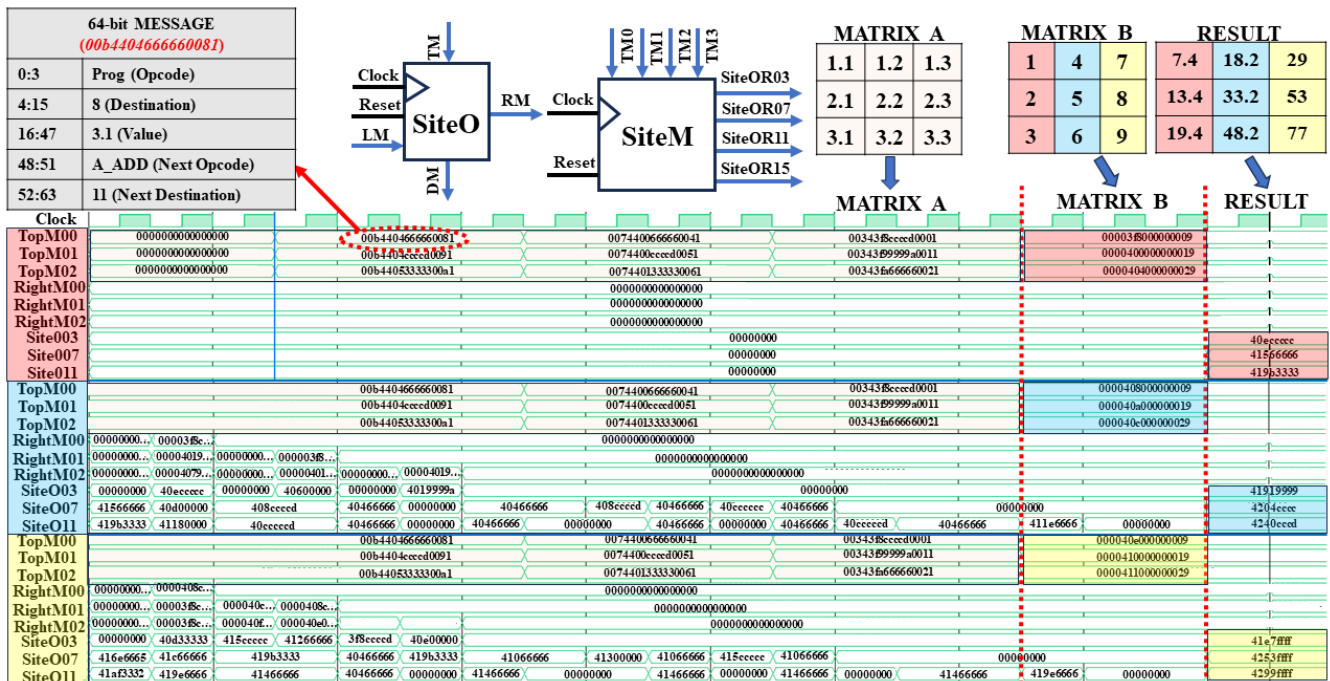


Figure 6 Simulation result of Matrix Multiplication between Matrix A (3 X 3) and Matrix B (3 X 3)

TABLE II
A Summary of Matrix Multiplication Approach between TPU [14], MEISSA [14], and m-IPU

TYPE	PROCESSING ELEMENT	RESOURCE UTILIZATION	SHAPE		METHOD	DATA LOAD		LATENCY
			Matrix A	Matrix B		Matrix A	Matrix B	
TPU	MAC	Multipliers: $N \times P$ Adders: $M \times P$	$N \times M$	$M \times P$	Systolic Array	Stored	Left to Right	$N + 2M + P - 2$
MEISSA	Multipliers & Adder Trees	Multipliers: $M \times P$ Adders: $P \times (M - 1)$	$N \times M$	$M \times P$	Systolic Array	Stored	Left to Right	$N + M + P + \log(M) - 2$
m-IPU	SiteO	SiteOs: $\{(N \times M) + N\} \times P$	$N \times M$	$M \times P$	Messaging-based	Program	Vertical Bus	$N + P + 2$

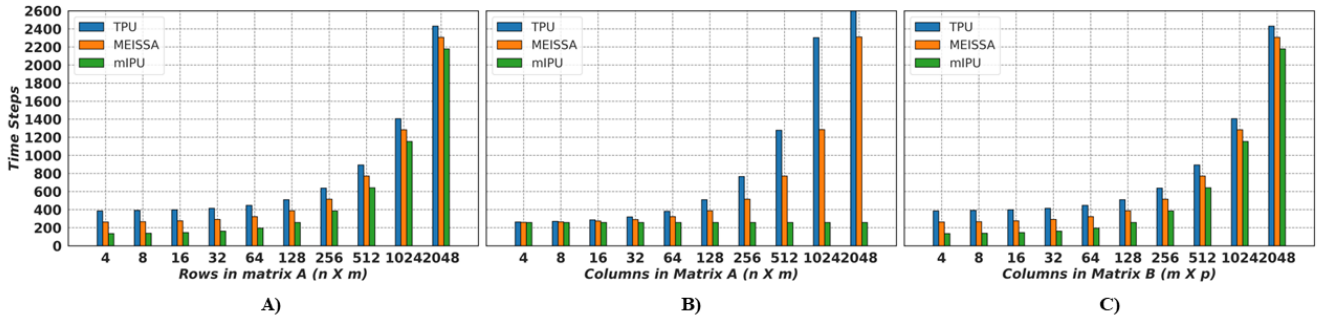


Figure 7 Comparison of the total time steps for matrix multiplication when A) n varies from 2 to 2048, $m = 128$, $p = 128$, B) m varies from 2 to 2048, $n = 128$, and $p = 128$, and c) p varies from 2 to 2048, $n = 128$, $m = 128$.

Table III
m-IPU (SiteM) Design parameters

Technology	TSMC 28nm		
Process	HPC+		
Metal Layer	1P8M		
Voltage (V_{DD})	0.9V (nominal)		
Package	Wire Bond		
Frequency	100 MHz		
Power (mW)	Leakage	Dynamic	Total
	0.42	44.08	44.5
Cell Count	Sequential	Inverter	Logic
	25692	4203	64305
			Total
			94200

Design optimization constraints define timing and area optimization goals for Cadence Genus. We specify these constraints. Genus optimizes the synthesis of the design by these constraints, but not at the expense of the design rule constraints. That is, Genus never attempts to violate the higher-priority design rules. We had to modify the design constraint several times to meet the design requirements. After performing the synthesis, we performed functional verification with the synthesized netlist to confirm that the synthesis tool has not altered the functionality. The throughput calculation of convolution operations utilizing available hardware resources is appended in Algorithm 1 of the Appendix section as supplementary file. We have measured the throughput for both 2D (Gray Image) and 3D (Color Image) convolution and during our observation, we varied both image and filter sizes. We have considered 32 data batches where each batch contains 128 images with 100 MHz clock frequency and 4096 available SiteOs. The padding and stride are kept 0 and 1 in both cases. For 3D convolution, we assumed that 64 filters are involved in the convolution process.

A. Evaluation

To verify our matrix-matrix multiplication approach, we have simulated our design with numerous values, however, a matrix-matrix multiplication between matrix A (3X3) and matrix B (3X3) is appended in Figure 6 for demonstrating our matrix-matrix multiplication process. Here, 9 messages are sent initially at 3 different steps to program 9 SiteOs with matrix A. In this stage, data reach to respective SiteOs through hopping. After that, each column of matrix B is passed to the m-IPU using vertical bus for multiplication. Once the multiplication is finished, results are sent to the desired SiteO for addition. This process is repeated until all columns are transferred and finally results are collected.

Table II summarizes the key characteristics including processing element, resource utilization, latency of matrix multiplication approaches between matrix A ($N \times M$) and matrix B ($M \times P$) in three different hardware accelerators (TPU, MEISSA, m-IPU). Both TPU and MEISSA utilize systolic array to perform matrix multiplication whereas our design incorporates messaging-based intelligent dataflow mechanism to program hardware at run-time. The latency of our matrix-matrix multiplication unit has been observed varying different (rows and columns) dimensions of matrix A and matrix B. Figure 7 (A), (B), and (C) represents the comparison of latency among MEISSA, TPU, and our design by varying N , M , and P individually from 4 to 2048 keeping other two parameters constant (128). In all cases, m-IPU outperforms the remaining two state-of-the-art matrix multiplication architectures.

Besides, we evaluate power consumption and resource utilization under TSMC 28nm technology to demonstrate our architecture's efficiency. The key design parameters of the m-IPU architecture are listed in Table III that indicates the design

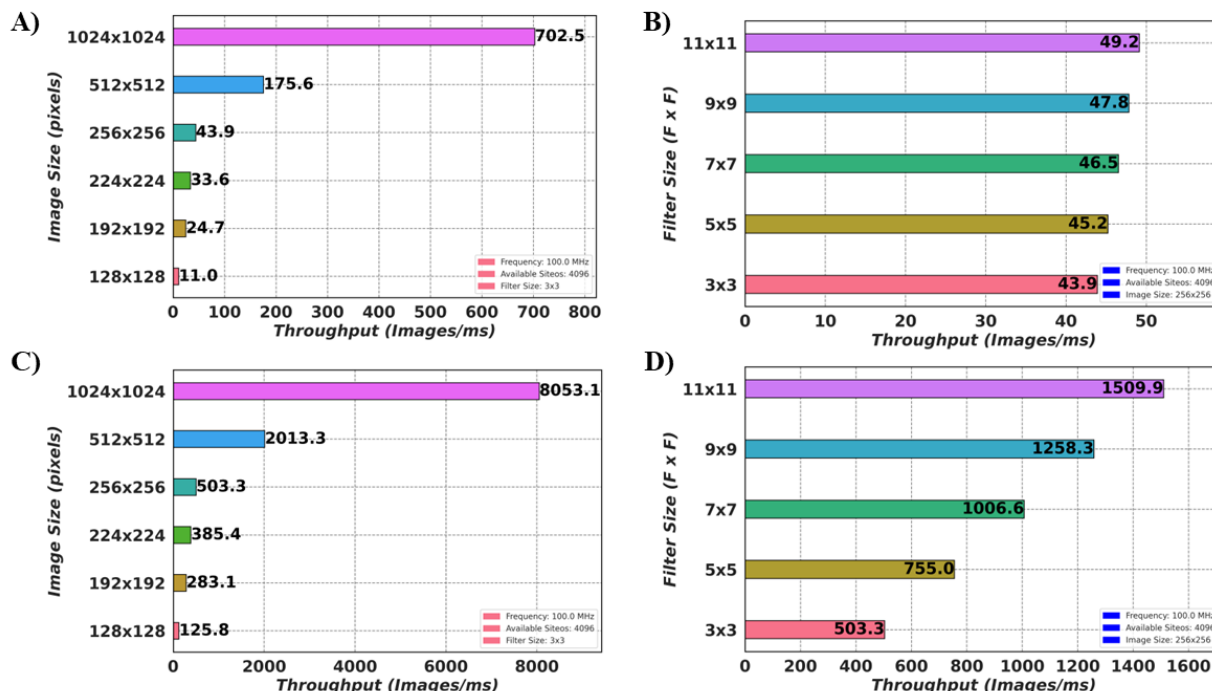


Figure 8 Throughput measurement by varying A) Image Size B) Filter Size for 2D Convolution and C) Image Size D) Filter Size for 3D Convolution.

consumes only 44.08 mW dynamic power at 0.9V operating voltage. The low dynamic power consumption suggests our design’s efficient task partitioning at runtime due to intelligent programmability and effective data mapping. Moreover, messages are loaded only from one direction (Top) and after multiplication the SiteOs transfer data through horizontal bus; as a result, m-IPU involves less signal transmission at runtime.

Next, we identify an effective data mapping strategy to accomplish faster convolution operation with less hardware resources. Finally, we benchmark our design by calculating throughput for multi-batch convolution operation. Figure 8(A) represents throughput varying image sizes from (128 X 128) to (1024 X 1024) maintaining a fixed filter size of (3 X 3) for 2D convolution. On the other hand, figure 8(B) highlights throughput for 2D convolution for different filter sizes (from 3 X 3 to 11 X 11) while keeping a fixed image dimension of (256 X 256). Our methodology completes 2D convolution operation of (32 X 128) images of size (1024 X 1024) with a filter of size (3 X 3) utilizing 4096 SiteOs and 100 MHz frequency within just 702.5 milliseconds. Again, the time required to execute a 2D convolution operation for (32 X 128) images of dimension (256 X 256) using a (11 X 11) filter keeping the other parameters unchanged is only 49.2 milliseconds. Similarly, figure 8 (C) and 8 (D) demonstrates the throughput for 3D convolution varying image and filter size respectively. Here, we have only considered the throughput for convolution operation as it consumes major time of the entire network and omitted the data loading and feed forward network time during benchmarking. Further validation, benchmarking, and identifying better data mapping algorithm are part of our ongoing work.

VI. CONCLUSION

The trend of deploying machine learning and deep learning algorithms in widespread applications necessitates an efficient hardware accelerator for executing matrix multiplication operation within a limited hardware budget. To do so, developing a unified hardware architecture that features reconfigurability, low-power, low-latency, and high-throughput is essential. In this work, we presented an innovative messaging-based computing paradigm that inherently programs hardware units at runtime. In addition to this, we proposed an ultra-low-latency matrix multiplier that outperforms existing systolic array-based matrix multiplication architecture such as TPU and MEISSA. Our design has been validated through simulations under TSMC 28nm technology. We have also established a methodology to benchmark convolution operation utilizing available hardware resources and achieved high throughput. Our future work will explore embedding of mIPU in RISC-V based SoC platforms such as Rocket chip[64] or Parrot 0.

REFERENCES

- [1] A. Krizhevsky, I. Sutskever, and G. E. Hinton, “ImageNet Classification with Deep Convolutional Neural Networks,” *Communications of the ACM*, vol. 60, no. 6, pp. 84–90, May 2012
- [2] K. Simonyan and A. Zisserman, “Very Deep Convolutional Networks for Large-Scale Image Recognition,” *Computer Vision and Pattern Recognition*, Sep. 2014.
- [3] C. Szegedy *et al.*, “Going deeper with convolutions,” *2015 IEEE Conference on Computer Vision and Pattern Recognition (CVPR)*, Boston, MA, USA, 2015, pp. 1–9.
- [4] K. He, X. Zhang, S. Ren and J. Sun, “Deep Residual Learning for Image Recognition,” *2016 IEEE Conference on Computer Vision and Pattern Recognition (CVPR)*, Las Vegas, NV, USA, 2016, pp. 770–778.

- [5] S. Hochreiter and J. Schmidhuber, "Long Short-Term Memory," *Neural Computation*, vol. 9, no. 8, pp. 1735–1780, Nov. 1997.
- [6] Chung, Junyoung, et al. "Empirical Evaluation of Gated Recurrent Neural Networks on Sequence Modeling." ArXiv.org, 2014, arxiv.org/abs/1412.3555.
- [7] A. Vaswani et al., "Attention Is All You Need," arXiv.org, Jun. 12, 2017. <https://arxiv.org/abs/1706.03762>.
- [8] R. H. Dennard, F. H. Gaensslen, H. -N. Yu, V. L. Rideout, E. Bassov and A. R. LeBlanc, "Design of ion-implanted MOSFET's with very small physical dimensions," in *IEEE Journal of Solid-State Circuits*, vol. 9, no. 5, pp. 256-268, Oct. 1974
- [9] T. N. Theis and H. . -S. P. Wong, "The End of Moore's Law: A New Beginning for Information Technology," in *Computing in Science & Engineering*, vol. 19, no. 2, pp. 41-50, Mar.-Apr. 2017.
- [10] R. Hameed et al., "Understanding sources of inefficiency in general-purpose chips," *ACM SIGARCH Computer Architecture News*, vol. 38, no. 3, pp. 37–47, Jun. 2010.
- [11] J. L. Hennessy and D. A. Patterson, "A new golden age for computer architecture: Domain-specific hardware/software co-design, enhanced security, open instruction sets, and agile chip development," *2018 ACM/IEEE 45th Annual International Symposium on Computer Architecture (ISCA)*, Los Angeles, CA, USA, 2018, pp. 27-29.
- [12] N. P. Jouppi et al., "In-datacenter performance analysis of a tensor processing unit," *2017 ACM/IEEE 44th Annual International Symposium on Computer Architecture (ISCA)*, Toronto, ON, Canada, pp. 1-12, 2017
- [13] B. Asgari, R. Hadidi and H. Kim, "MEISSA: Multiplying Matrices Efficiently in a Scalable Systolic Architecture," *2020 IEEE 38th International Conference on Computer Design (ICCD)*, Hartford, CT, USA, pp. 130-137, 2020
- [14] Z. Zhang, H. Wang, S. Han and W. Dally, "SpArch: Efficient Architecture for Sparse Matrix Multiplication," in *2020 IEEE International Symposium on High Performance Computer Architecture (HPCA)*, San Diego, CA, USA, pp. 261-274, 2020.
- [15] N. Srivastava, H. Jin, J. Liu, D. Albonese and Z. Zhang, "MatRaptor: A Sparse-Sparse Matrix Multiplication Accelerator Based on Row-Wise Product," *2020 53rd Annual IEEE/ACM International Symposium on Microarchitecture (MICRO)*, Athens, Greece, pp. 766-780, 2020.
- [16] M. Liang, M. Chen, Z. Wang and J. Sun, "A CGRA based Neural Network Inference Engine for Deep Reinforcement Learning," *2018 IEEE Asia Pacific Conference on Circuits and Systems (APCCAS)*, Chengdu, China, 2018, pp. 540-543.
- [17] A. Gholami, Z. Yao, S. Kim, C. Hooper, M. W. Mahoney and K. Keutzer, "AI and Memory Wall," in *IEEE Micro*, vol. 44, no. 3, pp. 33-39, May-June 2024.
- [18] "Does AI have a hardware problem?" *Nature Electronics*, vol. 1, no. 4, pp. 205–205, Apr. 2018.
- [19] J. Welsler, J. W. Pitera and C. Goldberg, "Future Computing Hardware for AI," *2018 IEEE International Electron Devices Meeting (IEDM)*, San Francisco, CA, USA, 2018, pp. 1.3.1-1.3.6.
- [20] V. Sze, Y.-H. Chen, T.-J. Yang, and J. S. Emer, *Efficient Processing of Deep Neural Networks*. Cham: Springer International Publishing, 2020.
- [21] J. Leskovec, L. A. Adamic, and B. A. Huberman, "The Dynamics of Viral Marketing," *Trans. on the Web (TWEB)*, 2007.
- [22] Autel, Autel X-Star Quadcopter, 2020 (accessed March 15, 2024). [Online]. Available: <https://www.autelrobotics.com/x-star-camera-drone>.
- [23] T. Nowatzki, V. Gangadhan, K. Sankaralingam and G. Wright, "Pushing the limits of accelerator efficiency while retaining programmability," *2016 IEEE International Symposium on High Performance Computer Architecture (HPCA)*, Barcelona, Spain, 2016, pp. 27-39.
- [24] M. Duranton, K. D. Bosschere, C. Gamrat, J. Maebe, H. Munk, and O. Zendra. 2017. The HiPEAC Vision 2017. In *Proceedings of the European Network of Excellence on High Performance and Embedded Architecture and Compilation*.12.
- [25] R. Tessier, K. Pocek and A. DeHon, "Reconfigurable Computing Architectures," in *Proceedings of the IEEE*, vol. 103, no. 3, pp. 332-354, March 2015.
- [26] Z. Li, D. Wijerathne, and T. Mitra, "Coarse Grained Reconfigurable Array (CGRA)." Available: <https://www.comp.nus.edu.sg/~tulika/CGRA-Survey.pdf>.
- [27] Ian Kuon; Russell Tessier; Jonathan Rose, *FPGA Architecture: Survey and Challenges*, 2008.
- [28] H. Xiao, X. Hu, T. Gao, Y. Zhou, S. Duan and Y. Chen, "Efficient Low-Bit Neural Network with Memristor-Based Reconfigurable Circuits," *IEEE Transactions on Circuits and Systems II: Express Briefs*, vol. 71, no. 1, pp. 66-70, Jan. 2024.
- [29] Md Arif Iqbal, Srinivas Rahul Sapireddy, S. Dasari, Kazi Asifuzzaman, and M. Rahman, "A review of crosstalk polymorphic circuits and their scalability," *Memories - Materials Devices Circuits and Systems*, vol. 7, pp. 100094–100094, Apr. 2024.
- [30] N. K. Macha, B. T. Repalle, M. A. Iqbal and M. Rahman, "Crosstalk-Computing-Based Gate-Level Reconfigurable Circuits," in *IEEE Transactions on Very Large-Scale Integration (VLSI) Systems*, vol. 30, no. 8, pp. 1073-1083, Aug. 2022.
- [31] P. Samant, Naveen Kumar Macha, and M. Rahman, "A Neoteric Approach for Logic with Embedded Memory Leveraging Crosstalk Computing," *ACM Journal on Emerging Technologies in Computing Systems*, vol. 19, no. 1, pp. 1–16, Dec. 2022.
- [32] A. Podobas, K. Sano and S. Matsuoka, "A Survey on Coarse-Grained Reconfigurable Architectures from a Performance Perspective," in *IEEE Access*, vol. 8, pp. 146719-146743, 2020.
- [33] L. Liu et al., "A Survey of Coarse-Grained Reconfigurable Architecture and Design," *ACM Computing Surveys*, vol. 52, no. 6, pp. 1–39, Oct. 2019.
- [34] Bingfeng Mei, S. Vernalde, D. Verkest, H. De Man and R. Lauwereins, "Exploiting loop-level parallelism on coarse-grained reconfigurable architectures using modulo scheduling," *2003 Design, Automation and Test in Europe Conference and Exhibition*, Munich, Germany, 2003, pp. 296-301.
- [35] Fava, L. B. R. V. (2024). CGRA-based Deep Neural Network for Object Identification. Instituto Superior Técnico.
- [36] M. Wijtvljet, L. Waeijen and H. Corporaal, "Coarse grained reconfigurable architectures in the past 25 years: Overview and classification," *2016 International Conference on Embedded Computer Systems: Architectures, Modeling and Simulation (SAMOS)*, Agios Konstantinos, Greece, 2016, pp. 235-244.
- [37] M. Tanomoto, S. Takamaeda-Yamazaki, J. Yao and Y. Nakashima, "A CGRA-Based Approach for Accelerating Convolutional Neural Networks," *2015 IEEE 9th International Symposium on Embedded Multicore/Many-core Systems-on-Chip*, Turin, Italy, 2015, pp. 73-80.
- [38] Y. Liang, J. Tan, Z. Xie, Z. Chen, D. Lin, and Z. Yang, "Research on Convolutional Neural Network Inference Acceleration and Performance Optimization for Edge Intelligence," *Sensors*, vol. 24, no. 1, p. 240, Jan. 2024.
- [39] . Ando, S. Takamaeda-Yamazaki, M. Ikebe, T. Asai, and M. Motomura, "A Multithreaded CGRA for Convolutional Neural Network Processing," *Circuits and Systems*, vol. 8, no. 6, pp. 149–170, Jun. 2017.
- [40] S. Yin et al., "A 1.06-to-5.09 TOPS/W reconfigurable hybrid-neural-network processor for deep learning applications," *2017 Symposium on VLSI Circuits*, Kyoto, Japan, 2017, pp. C26-C2.
- [41] Y. Wang et al., "Benchmarking the Performance and Energy Efficiency of AI Accelerators for AI Training," *2020 20th IEEE/ACM International Symposium on Cluster, Cloud and Internet Computing (CCGRID)*, Melbourne, VIC, Australia, 2020, pp. 744-751.
- [42] Y. -H. Chen, T. Krishna, J. S. Emer and V. Sze, "Eyeriss: An Energy-Efficient Reconfigurable Accelerator for Deep Convolutional Neural Networks," in *IEEE Journal of Solid-State Circuits*, vol. 52, no. 1, pp. 127-138, Jan. 2017.
- [43] Y.-H. Chen, T.-J. Yang, J. Emer, and V. Sze, "Eyeriss v2: A Flexible Accelerator for Emerging Deep Neural Networks on Mobile Devices," *arXiv.org*, May 20, 2019.
- [44] H. Kwon, A. Samajdar and T. Krishna, "Rethinking NoCs for spatial neural network accelerators," *2017 Eleventh IEEE/ACM International Symposium on Networks-on-Chip (NOCS)*, Seoul, Korea (South), 2017, pp. 1-8.
- [45] L. Liu, Z. Li, C. Yang, C. Deng, S. Yin and S. Wei, "HrEA: An Energy-Efficient Embedded Dynamically Reconfigurable Fabric for 13-Dwarfs Processing," in *IEEE Transactions on Circuits and Systems II: Express Briefs*, vol. 65, no. 3, pp. 381-385, March 2018.
- [46] R. Prabhakar et al., "Plasticine: A reconfigurable architecture for parallel patterns," *2017 ACM/IEEE 44th Annual International Symposium on Computer Architecture (ISCA)*, Toronto, ON, Canada, 2017, pp. 389-402.
- [47] O. Akbari, M. Kamal, A. Afzali-Kusha, M. Pedram and M. Shafique, "PX-CGRA: Polymorphic approximate coarse-grained reconfigurable architecture," *2018 Design, Automation & Test in Europe Conference & Exhibition (DATE)*, Dresden, Germany, 2018, pp. 413-418.
- [48] L. Duch, S. Basu, M. Peón-Quirós, G. Ansaloni, L. Pozzi and D. Atienza, "i-DPs CGRA: An Interleaved-Datapaths Reconfigurable Accelerator for

- Embedded Bio-Signal Processing," in *IEEE Embedded Systems Letters*, vol. 11, no. 2, pp. 50-53, June 2019.
- [49] M. Mishra, T. J. Callahan, T. Chelcea, G. Venkataramani, S. C. Goldstein, and M. Budi, "Tartan," *ACM SIGOPS Operating Systems Review*, vol. 40, no. 5, pp. 163-174, Oct. 2006.
- [50] J. D. Souza, L. Carro, M. B. Rutzig and A. C. S. Beck, "A reconfigurable heterogeneous multicore with a homogeneous ISA," *2016 Design, Automation & Test in Europe Conference & Exhibition (DATE)*, Dresden, Germany, 2016, pp. 1598-1603.
- [51] T. Chen, S. Srinath, C. Batten and G. E. Suh, "An Architectural Framework for Accelerating Dynamic Parallel Algorithms on Reconfigurable Hardware," *2018 51st Annual IEEE/ACM International Symposium on Microarchitecture (MICRO)*, Fukuoka, Japan, 2018, pp. 55-67.
- [52] D. Voitsechov, O. Port and Y. Etsion, "Inter-Thread Communication in Multithreaded, Reconfigurable Coarse-Grain Arrays," *2018 51st Annual IEEE/ACM International Symposium on Microarchitecture (MICRO)*, Fukuoka, Japan, 2018, pp. 42-54.
- [53] C. Xu and J. McAuley, "A Survey on Dynamic Neural Networks for Natural Language Processing," *arXiv.org*, Feb. 24, 2023. <https://arxiv.org/abs/2202.07101>.
- [54] T. Bjerregaard and S. Mahadevan, "A survey of research and practices of Network-on-chip," *ACM Computing Surveys*, vol. 38, no. 1, p. 1, Jun. 2006.
- [55] M. Rahman, A. Iqbal, and S. Rahul, "A Messaging based Intelligent Computing Approach for Machine Learning Applications." Accessed: Mar. 20, 2024. [Online]. Available: <https://computing-lab.com/wp-content/uploads/2022/02/mIPU-v1.pdf>.
- [56] T. Wiatowski and H. Bölskei, "A Mathematical Theory of Deep Convolutional Neural Networks for Feature Extraction," in *IEEE Transactions on Information Theory*, vol. 64, no. 3, pp. 1845-1866, March 2018.
- [57] A. Gupta, K. Illanko and X. Fernando, "Object Detection for Connected and Autonomous Vehicles using CNN with Attention Mechanism," *2022 IEEE 95th Vehicular Technology Conference: (VTC2022-Spring)*, Helsinki, Finland, 2022, pp. 1-6.
- [58] Y. Li, J. Luo, S. Deng and G. Zhou, "CNN-Based Continuous Authentication on Smartphones with Conditional Wasserstein Generative Adversarial Network," in *IEEE Internet of Things Journal*, vol. 9, no. 7, pp. 5447-5460, 1 April 2022.
- [59] D. R. Sarvamangala and R. V. Kulkarni, "Convolutional neural networks in medical image understanding: a survey," *Evolutionary Intelligence*, vol. 15, Jan. 2021.
- [60] J. Guo, H. -T. Nguyen, C. Liu and C. C. Cheah, "Convolutional Neural Network-Based Robot Control for an Eye-in-Hand Camera," in *IEEE Transactions on Systems, Man, and Cybernetics: Systems*, vol. 53, no. 8, pp. 4764-4775, Aug. 2023.
- [61] V. Sharma, M. Gupta, A. Kumar, and D. Mishra, "Video Processing Using Deep Learning Techniques: A Systematic Literature Review," in *IEEE Access*, vol. 9, pp. 139489-139507, 2021.
- [62] S. Yang, "Natural Language Processing Based on Convolutional Neural Network and Semi Supervised Algorithm in Deep Learning," *2022 International Conference on Artificial Intelligence in Everything (AIE)*, Lefkosa, Cyprus, 2022, pp. 174-178.
- [63] O. Abdel-Hamid, A. -r. Mohamed, H. Jiang, L. Deng, G. Penn and D. Yu, "Convolutional Neural Networks for Speech Recognition," in *IEEE/ACM Transactions on Audio, Speech, and Language Processing*, vol. 22, no. 10, pp. 1533-1545, Oct. 2014.
- [64] K. Asanović *et al.*, "The Rocket Chip Generator," 2016. Available: <https://www2.eecs.berkeley.edu/Pubs/TechRpts/2016/EECS-2016-17.pdf>.
- [65] D. Petrisko *et al.*, "BlackParrot: An Agile Open-Source RISC-V Multicore for Accelerator SoCs," *IEEE Micro*, vol. 40, no. 4, pp. 93-102, Jul. 2020.



Md. Rownak Hossain Chowdhury, received the B.Sc. degree in electrical and electronic engineering from Khulna University of Engineering and Technology, Khulna, Bangladesh, in 2010. He is currently pursuing the Ph.D. degree with the Department of Electrical and Computer Engineering, University of Missouri-Kansas City, Kansas City, MO, USA. His current research interests focus on developing innovative computing techniques for AI hardware accelerator.



Mostafizur Rahman, received the Ph.D. degree in electrical and computer engineering from the University of Massachusetts Amherst, Amherst, MA, USA.

He was with the Department of Computer Science and Electrical Engineering (CSEE), University of Missouri-Kansas City, Kansas City, MO, USA, where he leads the Nanoscale Integrated Circuits Laboratory and is currently a Co-Lead for the Center for Interdisciplinary Nanoscale Research. His group's research focuses on transformative approaches for nanoelectronics to surpass the current limitations of today's integrated circuits.

Dr. Rahman is currently the Publication Chair for NANOARCH and a Guest Editor for special issue of the *IEEE Transactions on Nanotechnology*. He is also a Program Committee Member for NANOARCH and VLSI design conferences. He is currently a Reviewer for the *IEEE Transactions on Nanotechnology*, *ACM Journal on Emerging Technologies in Computing Systems*, the Journal of Parallel and Distributed Computing, NANOARCH, and other publications.